Computers in Industry 133 (2021) 103550

Contents lists available at ScienceDirect

Computers in Industry

journal homepage: www.elsevier.com/locate/compind

A computer vision based online quality control system for textile yarns

Noman Haleem*,[1], Matteo Bustreo, Alessio Del Bue

Pattern Analysis & Computer Vision, Istituto Italiano di Tecnologia, Via Enrico Melen 83, Genova 16152, Italy

ARTICLE INFO

Article history:
Received 24 May 2021
Received in revised form 16 September 2021
Accepted 21 September 2021
Available online xxxx

Keywords:
Image acquisition
Computer vision
Textile yarn
Online quality control
Viola-Jones algorithm
Yarn spinning

ABSTRACT

Yarn quality control is a crucial step in producing high quality textile end products. Online yarn testing can reduce latency in necessary process control by providing rapid insights into yarn quality, leading to production of superior quality yarns. However, both widely used capacitance based evenness testers and emerging imaging based evenness testing systems are largely offline in operation (i.e. a posteriori). A suitable online system that could be employed to test quality of a variety of yarns in normal industrial processing conditions does not yet exist.

In this study, we propose an online evenness testing system for measurement of a certain type of yarn defect called nep by using imaging and computer vision techniques. The developed system directly captures yarn images on a spinning frame and uses Viola-Jones object detection algorithm for real-time detection of nep defects. The validation of nep detection algorithms and comparison of the new method with an existing evenness tester in terms of nep count demonstrated its reasonable defect detection accuracy and promising potential for application in wider yarn spinning industry.

1. Introduction

Yarn quality is an umbrella term for a number of physical properties of yarns, the most critical of which is yarn evenness i.e. the uniformity of fibre mass distribution along yarn length (Slater, 1986). A significant variation in fibre mass appears as a noticeable defect on yarn surface and undermines its mechanical performance, which causes excessive end breakages both within yarn spinning and in down stream textile processing. Uneven yarns deteriorate fabric appearance by producing undesired geometrical patterns and through variation in shade due to irregular dye uptake (Srinivasan et al., 1992; Shamey and Hussain, 2005). The poor quality fabrics are often rejected by customers causing financial loss and product wastage.

Yarn evenness related defects can be broadly classified into thick places (accumulation of fibres mass relative to yarn diameter), thin places (reduction of fibre mass relative to yarn diameter) and neps (entangled fibrous mass), each of which is further categorised into various subclasses based on defect length and diameter (Kretzschmar and Furter, 2008). The complete eradication of yarn defects is not practically possible as their origins lie in both raw material characteristics and fibre processing parameters but their extent could be minimised through effective process control and timely machine maintenance. This approach essentially requires rapid or live insights into yarn quality during its production at individual spindle level i.e. online testing but currently yarn evenness testers can only evaluate yarn quality after its production i.e. offline testing. The existing yarn evenness testers, which can be categorised into laboratory scale and modular testing units deployed on winding machines, often work on capacitive sensing principle, where variations in a narrow capacitance field caused by yarn mass irregularities are recorded as indirect measurement of yarn evenness (Uster, 12.05.2021; Uster Quantum, 25.08.2021). The laboratory scale evenness testing is a destructive test and only a limited yarn sample from few randomly selected bobbins is generally tested from a population of several hundreds to few thousands of bobbins, produced in a single spinning cycle on a spinning frame. While this practice provides an overall picture of yarn quality at the level of spinning machine, it does not capture crucial quality insights at individual spindle level. The modular type evenness testers scan yarns during winding process and trigger a cutter and splicer assembly to physically cut any defected regions to avoid their propagation in end products. The yarn quality insights achieved on a winding machine cannot be directly used to control spinning process at spindle level due to lack of suitable means to trace individual yarns back to the spindles where they were produced.

* Corresponding author.
E-mail address: nomanhaleem@gmail.com (N. Haleem).
[1] Present address: Postboks 61, Medisinsk Avdeling, Haukeland universitetssjukehus, Jonas Lies Vei 65, 5021, Bergen, Norway.

https://doi.org/10.1016/j.compind.2021.103550
0166-3615/

Recently, image processing has emerged as a potent method for evaluating yarn quality as several studies reported application of image processing algorithms to measure yarn evenness (Badehnoush and Yazdi, 2012; Qin et al., 2010; Weigang, 2011; Koganeya et al., 2012; Gonçalves et al., 2012; Carvalho et al., 2013; Roy et al., 2013; Roy et al., 2013; Zhong et al., 2014; Gonçalves et al., 2015; Li et al., 2015; Sengupta et al., 2015; Li et al., 2016; Roy et al., 2017; Roy et al., 2018; Pinto et al., 2019). These algorithms generally worked by first segmenting yarn body from background using image filtering (Gonçalves et al., 2012; Zhong et al., 2014; Gonçalves et al., 2015), edge detection (Roy et al., 2013; Roy et al., 2013; Sengupta et al., 2015), spatial transformation (Gonçalves et al., 2012; Gonçalves et al., 2015), morphological operations (Pinto et al., 2019) and clustering techniques (Li et al., 2015; Li et al., 2016). This was followed by segmenting yarn core from surrounding hair fibres through grayscale thresholding (Koganeya et al., 2012; Gonçalves et al., 2012; Gonçalves et al., 2015; Li et al., 2016; Pinto et al., 2019), image binarization (Roy et al., 2013; Roy et al., 2013; Sengupta et al., 2015) and neighbourhood pixel operations (Li et al., 2015) to isolate yarn core. Yarn evenness was then determined by measuring the core diameter at various points along yarn length. It is important to note that almost all of these works were conducted in offline setting as they used images that were either taken from static yarn samples (Gonçalves et al., Pinto et al., 2019; Loresco et al., 2018) or from yarns moving on laboratory scale transport devices (Koganeya et al., 2012; Zhong et al., 2014; Sengupta et al., 2015; Li et al., 2016; Roy et al., 2018). Some researchers described the possibility of translating their laboratory scale systems to a spinning frame for online monitoring of yarn evenness but did not provide any further concrete studies on this subject (Roy et al., 2013; Roy et al., 2013; Li et al., 2016; Pinto et al., 2019). In only one study, a digital camera was actually deployed on a spinning frame but it recorded images of spinning triangle (i.e. a small fibrous zone where twist is inserted into fibrous stream) to indirectly measure yarn evenness (Badehnoush and Yazdi, 2012). While a strong correlation was noted between the width of the triangle and yarn evenness, the industrial application of this approach is limited due to several constraints associated with direct imaging of spinning triangle in a normal spinning process (Haleem et al., 2019). Two other studies that were aimed at online measurement of yarn evenness, instead employed CCD cameras on a roving machine and did not report its relevance with yarn evenness (Qin et al., 2010; Weigang, 2011). Hence, a suitable online yarn evenness tester remained non-existent.

In this study, we propose a new system for online measurement of yarn evenness to address the above described gap. An optimal image acquisition setup was developed to directly capture high quality yarn images in real-time yarn production. These images were used to train and validate computer vision algorithms to identify a certain type of yarn defect called nep. The new system was then employed in regular industrial production for online testing of different yarn varieties and the outcomes were validated through comparison with an existing commercial evenness tester.

2. Materials and methods

2.1. Yarn image acquisition

A Basler 1440–220 µm digital camera (Basler, Germany) fitted with a 50 mm lens (Tamron, Japan) and two extension rings of 5 mm thickness each, was deployed on a Marzoli MST Spin Tester ring frame (Marzoli, Italy). The camera was connected to a Dell Precision 7510 laptop (Dell, USA) through a USB 3 connection and imaging was controlled using Basler Pylon camera software suite (version 5.2.0). The physical distance between the camera and yarn specimen was 21 cm, which resulted in a vertical field of view of 1.2 cm length, along yarn axis. The digital resolution of the camera was set up at 1100 × 1080 pixels and its exposure time was set to 3 µs. The imaging speed (i.e. frames per second or FPS) was calculated for yarn specimens based on their delivery speed, as further explained in Section 3.1. A LED type light source GES-6 K-20-T (Genesi Lux, Italy) of 3600 lumens flux was applied to provide ample amount of illumination. Both camera and light source were mounted on two separate Manfrotto 244RC mounting arms (Manfrotto, Italy). This experimental setup is shown in Fig. 1.

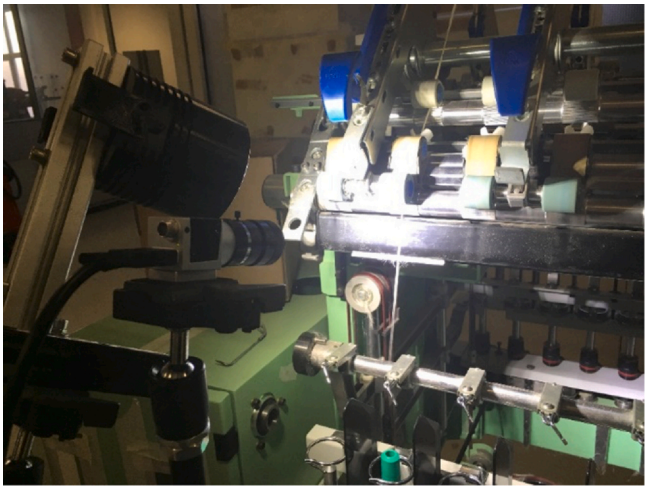

Fig. 1. Image acquisition system for online yarn imaging is mounted on a ring spinning frame.

2.2. Yarn spinning and yarn image dataset

Three textile yarns of linear densities 29.5 tex, 19.68 tex and 14.76 tex were produced using 590.5 tex Greek carded cotton roving (fibre length 30.7 mm & fibre fineness 0.175 tex). The yarn spinning speed was setup at 12,000 rpm and a spinning ring of 40 mm diameter was used. The ambient conditions in the spinning shed were maintained at 21.9 °C temperature and 51.3% relative humidity. The draft and twist settings for all three yarn varieties are given in Table 1.

For each yarn variety, 16 videos were recorded each of which contained 1750 continuous yarn images, resulting in a dataset of 84,000 images. To annotate these images as positive or negative, depending on occurrence or absence of nep defects respectively, a semi-automated approach based on a computer algorithm and an expert evaluator was used. The annotation algorithm that was developed in Python programming language, used OpenCV (computer vision) and NumPy libraries to process each image in the dataset by first thresholding the image based on grayscale intensity and then calculating the sum of all pixels in each row of the image. A nep often appears as a thick and obvious mass of fibres in normal yarn, which produces a sharp rise in row summation curve of yarn image. However, such a rise can also occur due to other sources of variations, i.e. excessive hairiness, accumulation of fluff or fly on yarn and other types of yarn defects. For this reason, an expert evaluator visually examined those images where a sharp increment occurred in row summation profile and marked those images as positives, where a nep was visually sighted. All other images in the dataset were marked as negative. The limited frequency of nep occurrences

Table 1
Spinning parameters for three varieties of yarns produced.

Yarn linear density (tex)	Total draft	Twist per meter
29.5	21.6	774.2
19.68	32.3	970.7
14.76	43.1	1092.5

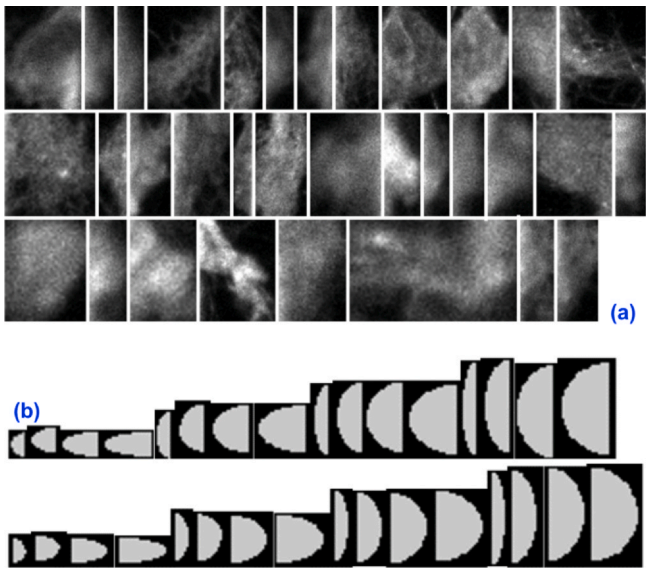

Fig. 2. Cropped (a) original & (b) synthetic nep images.

compared to normal yarn images resulted in an imbalanced yarn dataset i.e. low proportion of positive to negative images. The dataset was then split in training and validation sets in a ratio of 5:3, respectively.

2.3. Development of computer vision models for nep detection

Three computer vision models (termed as A, B & C) based on Viola-Jones algorithm were developed using OpenCV computer vision library in Python programming language. These models are essentially image classifiers, which varied in terms of the input data used in their training phase. The training data comprised of positive and negative images in 2:1 ratio and these images were rescaled at factors of 0.2 and 0.1, respectively to optimise training time. The number of training stages were 10 for each model.

In order to train Model A, 33 images of original neps were cropped out of positive images from training set, as shown in Fig. 2(a). Due to imbalanced dataset and lower number of nep images, data augmentation techniques based on linear image transformations i.e. scaling, translating and rotating were applied to produce 5000 nep images. These were combined with 2500 negative yarn images, also taken from the training set, and fed to the algorithm to train model A. For model B, similar augmentation strategy was applied on 32 'synthetic nep' images instead, which are computer generated images of half ellipses and vary in terms of major and minor axes length, as shown in Fig. 2(b). Lastly, a combination of both 33 original and 32 synthetic nep images was used to augment 5000 positive images to train model C.

2.4. Validation and testing

Nep detection models A, B & C were validated on a set of 200 yarn images, half of which contained exactly one nep and the other half did not contain any neps. The images classified as positive by computer vision models were marked as true positive if they also belonged to positive image class in the validation dataset, otherwise they were marked as false positive. Similarly, true and false negatives were determined by linking classification outcomes with negative image class of the dataset.

For online testing of nep detection system, the image acquisition assembly was deployed on spinning frame (as previously described in Section 2.1) and three yarns of 59.05, 29.5 & 14.76 tex linear densities were produced. Imaging was conducted on three specimens of each yarn type comprising of 250 m yarn length. A graphical interface based application was developed using Tkinter library in Python programming language, where Pypylon library (Basler, Germany) read camera output directly into the application and fed live image stream to computer vision models for nep detection. The detected neps were then classified into +140%, +200% and +400% subcategories based on thier average diameters, relative to normal yarn diameter. The exact same yarn specimens were then tested using Uster Tester 3 (Uster, Switzerland), which is an industrial standard for offline yarn evenness testing, for comparison and validation purposes.

3. Theory and calculation

3.1. Image acquisition on a spinning frame

During spinning process, yarn specimens rapidly rotate, oscillate and translate laterally under influence of spinning tension. The design of an online yarn imaging system need to take these dynamics into account to acquire optimal quality images suitable for processing and defect detection. The primary requirement of online yarn imaging is to capture sharp images that do not suffer from motion artefacts such as blurring, due to rapid movement of yarn specimen. This could be achieved by employing an ultra-low exposure time camera (i.e. exposure time in order of few micro seconds). However, such imaging arrangement would also require an external light source to provide substantial luminous flux as short shutter opening time would permit very limited amount of light, resulting in poor image contrast. Another camera setting that can supplement lightening conditions is digital gain, i.e. light sensitivity of camera sensor.

The optical components attached to camera need to meet two requirements as well i.e. optical resolution and size of the field of view. Both of these parameters are inversely proportional to each other as increasing one of them would compromise the other. Higher resolution exposes yarns in greater detail and potentially improves defect detection accuracy but also reduces the field of view, allowing yarn to possibly escape out of image frame due to its continuous lateral oscillations. A careful selection of optical components such as lens, extender rings, etc. is required to achieve substantial optical resolution in order of tens of micrometers and field of view in few centimetres to both effectively visualize yarn defects and adequately capture lateral motion of yarn specimens.

Finally, yarn specimens need to be imaged continually such that no yarn segment remain unrecorded. This is a critical requirement of any imaging based yarn testing system to ensure that all yarn length is scanned and can be achieved by synchronising imaging speed of the camera with yarn delivery rate, such that each yarn image would capture exactly consecutive yet non-overlapping yarn segments. The yarn imaging speed can be calculated as follows;

$$Frames\_per\_second = \frac{Yarn\_delivery\_speed}{Vertical\_field\_of\_view} \quad (1)$$

where,

$$Yarn\_delivery\_speed = \frac{Spindle\_speed}{Yarn\_twist\_level} \times Twist\_contraction\_factor \quad (2)$$

Based on nominal yarn delivery speed between 10 and 20 m /min on a ring spinning frame and a vertical field of view of few centimetre in length, the yarn imaging speed is expected to remain in order of few tens of images per second.

3.2. Computer vision models for nep detection

Neps appear as entangled fibrous objects in yarn images and the task of detecting them could be regarded as object detection problem in computer vision. However, an important consideration in selecting a suitable object detection method is high detection speed that could match imaging speed and yarn delivery rate. A comparison of various object detection methods shows that Viola-Jones algorithm provides high speed of object detection (up to 60 FPS) along with reasonable accuracy (Nguyen-Meidine et al., 2017). The same method has been successfully applied for other real-time applications and provided acceptable detection success rate (Keller et al., 2008; Castillo Salazar et al., 2019; Loresco et al., 2018).

Viola Jones method (Viola and Jones, 2001) works by efficiently extracting representative Haar features from input images using adaptive boosting technique. These features are used to train cascades of weak classifiers, whose weighted sum produce the final classifier used for object detection. A multi-stage detection approach is used on test images, where initial stages only apply few features on image window to determine the possible presence of the target object. If this test fails, the image is marked as negative and this strategy allows the algorithm to speedily detect target objects compared to other techniques. While it would be interesting to compare accuracy and speed of various object detection algorithms for nep detection, such an investigation is out of scope of the presented work and could be pursued in the future.

4. Results and discussion

4.1. Image acquisition

Fig. 3 shows three concatenated images of yarns with nep defects, acquired using the proposed image acquisition setup during yarn spinning process. Using the criteria of a suitable online yarn image as outlined in Section 3.1, the quality of the following image could be regarded as optimal and suitable for further image processing, based on (i) the absence of motion related blurring, (ii) substantial optical resolution that clearly visualizes nep defects and (iii) acceptable contrast between white yarn body and black background. In addition, an analysis of a series of continuous yarn images suggested that the size of the field of view was substantial to accommodate lateral oscillations of yarn during spinning process and all images represented consecutive yet non-overlapping yarn regions.

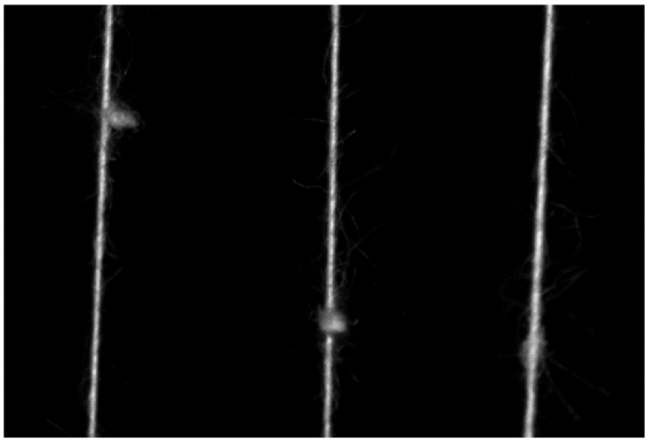

Fig. 3. An example yarn image with a nep defect taken using image acquisition system.

4.2. Validation of nep detection models

Three nep detection models i.e. A, B & C were validated using a validation dataset, which consisted of 100 positive (with neps) and 100 negative (without neps) yarn images. The classifications achieved by each model were categorised as true positive (TP), true negative (TN), false positive (FP) and false negative (FN). These parameters are provided for all three models in form of confusion matrices, as shown in Fig. 4, which suggest superior accuracy of Model C compared to both models A & B as it correctly classified 86% neps and 98% negative yarn images. In addition, its false positive and negative rates were 2% and 14% respectively.

In order to quantify the performance and facilitate inter-model comparison, four evaluation metrics, namely detection success rate (DSR), Sensitivity, Specificity and F-score, were calculated. The values of these metrics are provided in Table 2. The DSR characterises the ability of a classifier to accurately identify both positive and negative image classes. Sensitivity of a classifier is a ratio of correctly identified positive images to the total number of positive image detections while Specificity is a ratio of correctly identified negative images to the total number of negative identified images. The F-score is a cumulative representation of both sensitivity and specificity. A comparison of these metrics for all three models also suggests higher detection score, sensitivity, specificity and F-score value for Model C, making it a clear choice for online nep detection application.

Out of all three models, model A which was trained using original nep images showed most inferior performance metrics while model B, which was trained using synthetic nep images showed significantly superior results compared to model A but slightly lesser performance than model C. A closer look into inferior performance of model A points out a close resemblance between textures of neps and yarns as a potential reason for their underperformance. The similarly of textures is due to the fact that neps and yarns are made from the same fibrous materials and imaged exactly in the same way, hence, resulting in similar grayscale intensities of their constituting pixels. The Haar-like features calculated by the computer vision algorithm from both neps and yarns would be essentially similar, which limited the ability of Model A to effectively differentiate between neps and yarns resulting in both higher number of false positives and false negatives. Moreover, the shape of neps were highly irregular and did not serve as a differential metric for nep identification either. Two yarn image from validation of model A are shown in Fig. 5, which demonstrate excessive false detections on main yarn body due to inability of the model to differentiate between neps and yarn body. On the other hand, models B & C, both of which used synthetic nep images, were able to differentiate between neps and yarns as the grayscale intensity values of pixels lying within synthetic neps were uniform and clearly different than the normal yarns. In addition, their shape was also highly regular, which improved differentiation criteria between both groups.

4.3. Online testing of nep detection system

A comparison of online nep detection system (O) with Uster Tester 3 (U) is provided in Table 3, where each data point represents an average of 3 observations. The results show a substantial difference between both methods in terms of total number of neps and within nep sub classes. As a general trend, the number of neps detected by the online measurement technique are almost always higher than the number of neps reported by Uster tester in respective categories, except for + 140% neps category. However, the extent of this difference is particularly higher for coarser yarns (i.e. 59.05 tex) compared to finer yarns (i.e. 14.76 tex). The difference between total number of neps measured using both methods is also statistically significant as evaluated using Student's *T*-test (*P*-values:

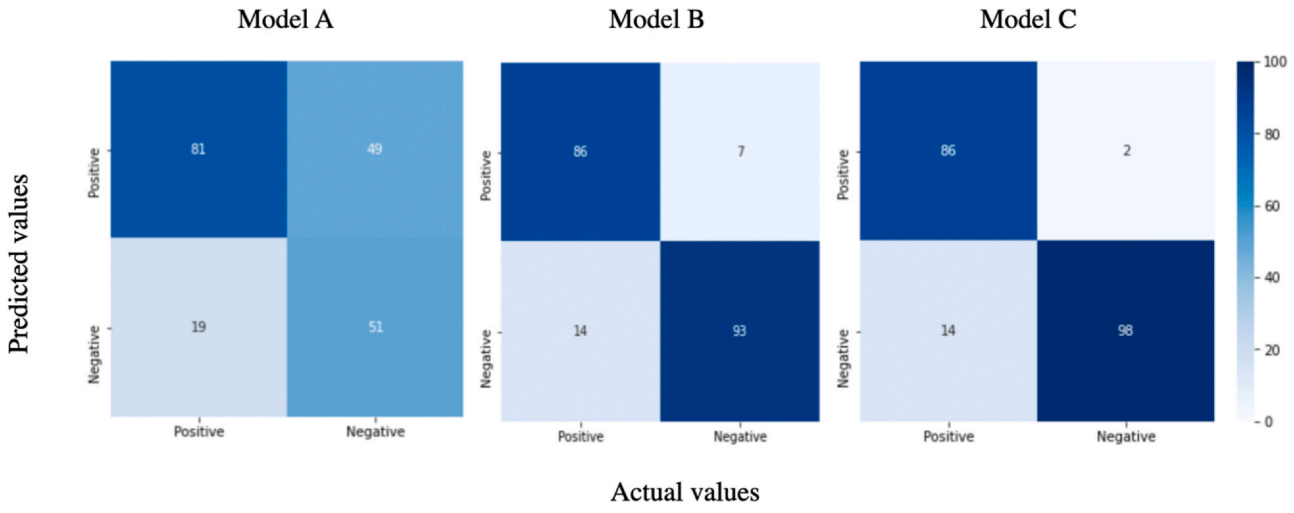

Fig. 4. Confusion matrices for all three nep detection models.

Table 2
Four valuation metrics as calculated for each nep detection model.

Model	DSR	Sensitivity	Specificity	F-score
A	0.66	0.81	0.51	0.62
B	0.9	0.86	0.93	0.89
C	0.92	0.86	0.98	0.91

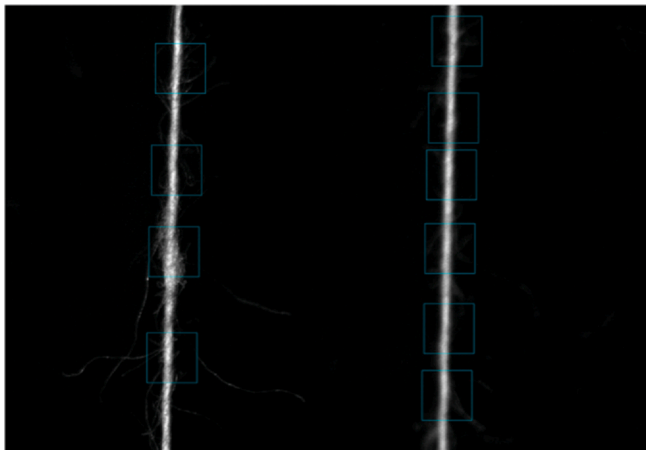

Fig. 5. Excessive false detections by Model A on a yarn image from validation dataset.

Table 3
A comparison of nep defect count as measured by Uster evenness tester (U) and Online yarn evenness measurement system (O).

Yarn linear density (tex)	140% neps		200% neps		400% neps		Total neps	
	U	*O*	*U*	*O*	*U*	*O*	*U*	*O*
59.05	5	146	3	11	3	0	11	157
29.5	26	256	5	45	0	2	31	303
14.76	220	193	56	132	3	20	278	346

59.05 tex yarn = 0.0002, 29.5 tex yarn = 0.0026, 14.76 tex yarn = 0.0032).

The contradictions in the nep measurements from both methods in terms of substantiality and statistical significance is particularly interesting because the results achieved from online evenness measurement system comes with an imagery evidence as all nep containing images were stored during testing. On the other hand, Uster Tester is a well-established industrial method for measurement of yarn evenness and associated defects. We expected a close agreement between measurements from both methods, which is clearly not the case. However, this discrepancy cannot be verified in current study as Uster Tester does not store images of yarn defects that could be directly compared with the online evenness testing system. We do not intend to undermine the accuracy of Uster Tester but the noted discrepancy essentially requires further controlled investigations as these differences could be attributed to two entirely different testing principles or a more complex underlying issue, which remains unclear at this point.

Other than this difference, the results achieved from imaging based evenness testing system indicate that our proposed system could be effectively used for online yarn testing and providing live insights into its quality for necessary process intervention and control, which can lead to production of superior quality yarns.

5. Conclusions

- An online yarn evenness testing system based on a combination of an image acquisition setup and Viola-Jones object detection algorithm is successfully developed to detect nep like defects during yarn production.
- The optimal quality online images of yarn could be acquired using an ultra-low exposure time imaging system combined with external illumination and suitable optical configuration.
- Viola-Jones algorithm effectively detected nep like defects in online yarn images with detection success rate of up to 92%, which may improve further with refinement of training strategy, size of training dataset or through experimenting with other object detection approaches.
- The count of nep defects achieved by online yarn evenness testing system was substantially higher than Uster Tester, although the trends of nep count were generally similar i.e. higher number of neps for finer yarns and vice versa.
- The substantial unexpected difference between nep count reported by online system and Uster tester may be attributed to two different testing principles but will essentially benefit from further careful investigations.
- In the future, the online yarn evenness measurement system can be used for detecting other types of yarn defects as well with necessary additions in image processing module to produce a complete yarn quality testing solution for wider yarn spinning industry.

CRediT authorship Contribution Statement

NH has performed experimental, data collection, programming, model development and analysis. He also drafted the work into a research publication. MB was involved in conceptualisation of online yarn evenness testing system and provided technical advice in image acquisition, processing and analysis. ADB provided administrative support in industrial collaboration and technical supervision of the project.

Declaration of Competing Interest

The authors declare that they have no known competing financial interests or personal relationships that could have appeared to influence the work reported in this paper.

Acknowledgement

We acknowledge research funding provided by Camozzi Group (Italy) for this research under Camozzi-IIT joint research laboratory initiative.

References

Badehnoush, A., Yazdi, A.Alameda, 2012. Real-time yarn evenness investigation via evaluating spinning triangle area changes. J. Text. Inst. 103, 850–861. https://doi.org/10.1080/00405000.2011.614741

Carvalho, V., Gonsalves, N., Soares, F., Vasconelos, R., Belsley, M., 2013. Yarn parameterization and fabric prediction using image processing. Text. Light Ind. Sci. Technol. 2, 6–12.⟨http://hdl.handle.net/1822/27424⟩.

Castillo Salazar, D.R., Gómez Alvarado, H.F., Guevara Maldonado, C.B., Lanzarini, L., 2019. Object detection application and Viola Jones algorithm for the development of a database in Alzheimer's patients. 14th Iberian Conference on Information Systems and Technologies ((CISTI)). pp. 1–7. https://doi.org/10.23919/CISTI.2019.8760869

Gonçalves, N., Carvalho, V., Belsley, M., Vasconcelos, R.M., Soares, F.O., Machado, J., 2015. Yarn features extraction using image processing and computer vision – a study with cotton and polyester yarns. Measurement 68, 1–15. https://doi.org/10.1016/j.measurement.2015.02.010

Gonçalves, N., Carvalho, V., Soares, F., Vasconcelos, R., 2012. Studies on the yarn mass parameters determination using Image Processing techniques. Proceedings of 2012 IEEE 17th International Conference on Emerging Technologies & Factory Automation (ETFA 2012). pp. 1–4. https://doi.org/10.1109/ETFA.2012.6489765

Haleem, N., Gordon, S., Liu, X., Hurren, C., Wang, X., 2019. Dynamic analysis of spinning triangle geometry part 1: validation of methodology. J. Text. Inst. 110, 660–670. https://doi.org/10.1080/00405000.2018.1511223

Keller, C.G., Sprunk, C., Bahlmann, C., Giebel, J., Baratoff, G., 2008. Real-time recognition of U.S. speed signs. 2008 IEEE Intell. Veh. Symp. 10, 518–523. https://doi.org/10.1109/IVS.2008.4621282

Koganeya, K., Yukishita, Y., Fujisaki, H., Jintoku, Y., Okuno, H., Fujigaki, M., 2012. Instrument for measuring the appearance width of running double ply staple yarn using lightness threshold for yarn image. Sen-I Gakkaishi 68, 98–105. https://doi.org/10.2115/fiber.68.98

Kretzschmar, S.D., Furter, R., 2008. Uster Classimat Quantum: Application report 6.

Li, Z., Pan, R., Wang, J., Wang, Z., Li, B., Gao, W., 2016. Real-time segmentation of yarn images based on an FCM algorithm and intensity gradient analysis. Fibres Text. Eastern Eur. 24, 45–50. https://doi.org/10.5604/12303666.1201130

Li, Z., Pan, R., Zhang, J., Li, B., Gao, W., Bao, W., 2015. Measuring the unevenness of yarn apparent diameter from yarn sequence images. Meas. Sci. Technol. 27, 015404. https://doi.org/10.1088/0957-0233/27/1/015404

Loresco, P.J., Valenzuela, I., Culaba, A., Dadios, E., 2018. Viola-Jones method of marker detection for scale-invariant calculation of lettuce leaf area, IEEE 10th international conference on humanoid, nanotechnology, information technology, communication and control. Environ. Manag. 1–5. https://doi.org/10.1109/HNICEM.2018.8666244

Nguyen-Meidine, L.T., Granger, E., Kiran, M., Blais-Morin, L., 2017. A comparison of CNN-based face and head detectors for real-time video surveillance applications. Seventh International Conference on Image Processing Theory Tools and Applications ((IPTA)). pp. 1–7. https://doi.org/10.1109/IPTA.2017.8310113

Pinto, R., Pereira, F., Carvalho, V., Soares, F., Vasconcelos, R., 2019. Yarn linear mass determination using image processing: first insights. IECON 2019 - 45th Annual Conference of the IEEE Industrial Electronics Society 198–203. https://doi.org/10.1109/IECON.2019.8926650

W. Qin , Q. Huang , G. Yang , Application of on-line yarn evenness measurement through CCD image sensors, 2010 International Conference on Computer Application and System Modeling (ICCASM 2010), (2010), pp. V6–112-V116–115. https://doi.org/10.1109/ICCASM.2010.5618988.

Roy, S., Sengupta, A., Maity, R., Sengupta, S., 2013. Yarn parameterization based on image processing, 2013 IEEE International Conference on Signal Processing. Computing and Control ((ISPCC)) 1–6. https://doi.org/10.1109/ISPCC.2013.6663391

Roy, S., Sengupta, A., Sengupta, S., 2013. Determination of the Diameter Spectrogram and Neps for Yarn Parameterization using Image Processing, International Journal of Electrical. Electron. Comput. Eng. 2 (2), 72–76.

Roy, S., Sengupta, A., Sengupta, S., 2017. Performance study of optical sensor for parameterization of staple yarn. Measurement 109, 394–407. https://doi.org/10.1016/j.measurement.2017.06.009

Roy, S., Sengupta, A., Sengupta, S., 2018. Quality testing of staple yarn by an instrument with dual sensing and its comparative study with capacitive sensing. Indian J. Fibre Text. Res. 43, 269–276.

Sengupta, A., Roy, S., Sengupta, S., 2015. Development of a low cost yarn parameterisation unit by image processing. Measurement 59, 96–109. https://doi.org/10.1016/j.measurement.2014.09.028

Shamey, R., Hussain, T., 2005. Critical solutions in the dyeing of cotton textile materials. Text. Prog. 37, 1–84. https://doi.org/10.1533/tepr.2005.0001

Slater, K., 1986. Yarn evenness. Text. Prog. 14, 1–90. https://doi.org/10.1080/00405168608688901

Srinivasan, K., Dastoor, P.H., Radhakrishnaiah, P., Jayaraman, S., 1992. FDAS: a knowledge-based framework for analysis of defects in woven textile structures. J. Text. Inst. 83, 431–448. https://doi.org/10.1080/00405009208631217

Uster Tester - staple yarn, accessed on 12.05.2021 at ⟨https://www.uster.com/en/instruments/staple-yarn-testing/uster-tester-staple-yarn/⟩.

Uster Quantum 4.0, accessed on 25.08.2021 at ⟨https://www.uster.com/en/uster-quantum-40/⟩.

Viola, P., Jones, M., 2001. Robust real-time object detection. Int. J. Comput. Vis. 4, 4.

Weigang, Q., 2011. On-line yarn evenness detection using CCD image sensor. On-line Yarn Evenness Detection Using CCD Image Sensor, 2011 Chinese Control and Decision Conference ((CCDC)). pp. 1787–1790. https://doi.org/10.1109/CCDC.2011.5968487

Zhong, P., Kang, Z., Han, S., Hu, R., Pang, J., Zhang, X., Huang, F., 2014. Evaluation method for yarn diameter unevenness based on image sequence processing. Tex. Res. J. 85, 369–379. https://doi.org/10.1177/0040517514547211